JACS
JOURNAL OF THE AMERICAN CHEMICAL SOCIETY

Article

Stereospecific Autocatalytic Surface Explosion Chemistry of Polycyclic Aromatic Hydrocarbons

Anais Mairena, Martin Wienke, Kévin Martin, Narcis Avarvari, Andreas Terfort, Karl-Heinz Ernst, and Christian Wäckerlin

J. Am. Chem. Soc., **Just Accepted Manuscript** • DOI: 10.1021/jacs.8b04191 • Publication Date (Web): 28 May 2018

ACS Publications

is published by the American Chemical Society. 1155 Sixteenth Street N.W., Washington, DC 20036

Stereospecific Autocatalytic Surface Explosion Chemistry of Polycyclic Aromatic Hydrocarbons

Anaïs Mairena[†], Martin Wienke[‡], Kévin Martin[§], Narcis Avarvari[§], Andreas Terfort[∥], Karl-Heinz Ernst[†,⊥,*] and Christian Wäckerlin[†,*]

[†] Empa - Swiss Federal Laboratories for Materials Science and Technology, 8600 Dübendorf, Switzerland

[‡] Department of Chemistry, University of Hamburg, 20146 Hamburg, Germany

[§] Laboratoire Moltech Anjou, Université d'Angers, Angers, France

[∥] Department of Chemistry, Institute of Inorganic and Analytical Chemistry, Goethe-University, 60438 Frankfurt, Germany

[⊥] Department of Chemistry, University of Zurich, 8057 Zurich, Switzerland

ABSTRACT: Autocatalytic processes are important in many fields of science, including surface chemistry. A better understanding of its mechanisms may improve the current knowledge on heterogeneous catalysis. The thermally-induced decomposition of eight different polycyclic aromatic hydrocarbons (PAHs) on a saturated monolayer of atomic oxygen on a Cu(100) surface is studied using temperature programmed reaction spectroscopy (TPRS), X-ray photoelectron spectroscopy (XPS) and scanning tunneling microscopy (STM). 9-bromo-heptahelicene decomposes autocatalytically in a narrow temperature range into CO_2 and H_2O, while non-halogenated heptahelicene decomposes into the same products but does not show autocatalytic behavior. Fixation of the hydrocarbon to the surface via the organometallic bond after elimination of the bromine is identified as prerequisite for the autocatalytic reaction mechanism. Of all hydrocarbons studied, only those being sterically overcrowded decompose autocatalytically. Such observation can be explained by facile dehydrogenation of the overcrowded PAHs. The reaction of such hydrogen with oxygen creates vacancies in the oxygen layer which catalyze as active sites further decomposition.

INTRODUCTION

Autocatalytic reactions are observed in many areas of chemistry, physics and biology, such as radical polymerization, nuclear chain reactions or protein-mediated biosynthesis.[1] The common figure of autocatalysis is the fact that a reaction product serves as catalyst. Therefore, the reaction rate is enhanced exponentially after initiation. Autocatalytic decomposition on surfaces that lead to desorption of the product in ultra-narrow temperature interval, coined as 'surface explosion',[2–4] have been observed for carboxylic acids on metal single crystals[5–10] as well as for NO + CO and NO + H_2 mixed layers on Pt(100).[11,12] A particularly well understood system is the thermally-induced decomposition of tartaric acid (TA) on Cu(110).[13] It was the first system to report chiral effects in a surface reaction.[14] Madix et al. realized that surface explosion requires the formation of vacancies in the closed-packed layer of molecules.[3] If a surface-adsorbed compound decomposes and the product leaves the surface, new empty surface sites (*) are created which catalyze further decomposition. For example:

$$HCOO^-(ads) + * \rightarrow CO_2 + \tfrac{1}{2}\, H_2 + 2\, * \qquad (1)$$

Initially, decomposition in a close packed monolayer of molecules is blocked due to the absence of vacancies. Therefore, a close-packed layer is stabilized beyond the temperature at which decomposition of an isolated species usually takes place.[15] Once initial decomposition starts at elevated temperatures, the production of vacancies autocatalytically enhance the reaction rate.

Coal has been used to reduce copper oxide into metallic copper for about 5000 years. For hydrocarbons adsorbed on well-defined model systems, such as a molecular monolayers (MLs) adsorbed on top of a layer of oxygen on copper single crystals, regular combustion into carbon dioxide and water has been observed.[16–20] Here, a stereospecific autocatalytic decomposition of polycyclic aromatic hydrocarbons (PAHs) on an oxygen covered Cu(100) surface is reported. The autocatalytic nature of the decomposition is based on vacancies created in the oxygen layer. It is observed that only non-planar bromin-

ated PAHs are burned in a surface explosion-style manner in a very narrow temperature range.

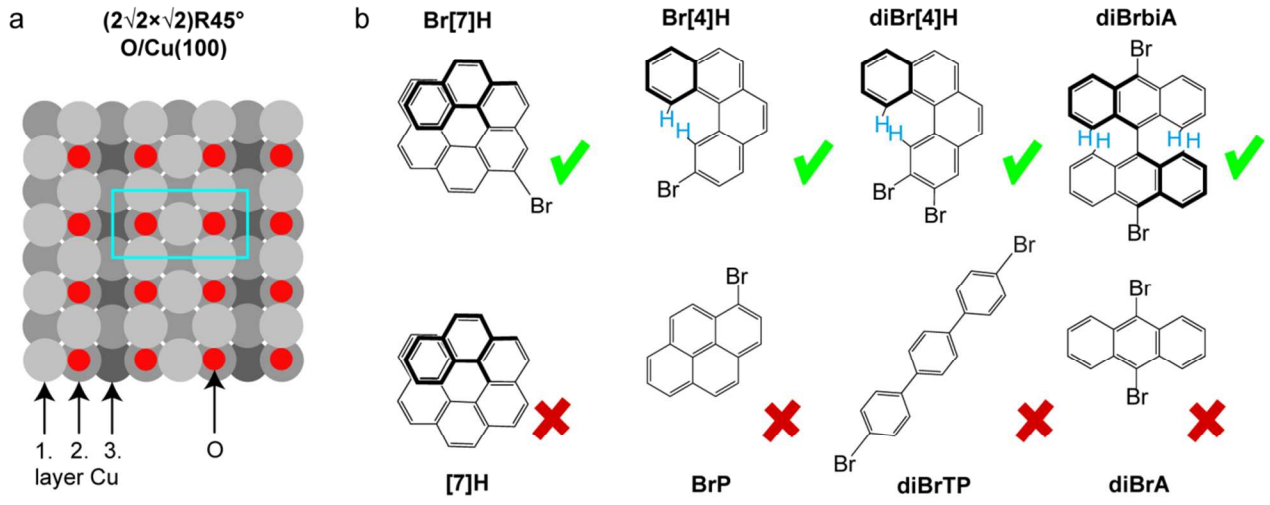

Figure 1. (a) Sketch of the (2√2×√2)R45° oxygen layer on Cu(100) and (b) structures of the studied PAHs. The molecules are: 9-bromo-heptahelicene (Br[7]H), heptahelicene ([7]H), 2-bromo-tetrahelicene (Br[4]H), 2,3-dibromo-tetrahelicene (diBr[4]H), 4,4'-dibromo-terphenyl (diBrTP), 1-bromo-pyrene (BrP), 10,10'-dibromo-9,9'-bisanthracene (diBrbiA), 9,10'-dibromo-anthracene (diBrA). Hydrogen atoms exposed to steric repulsion are highlighted in blue. Green ticks indicate autocatalytic decomposition of the saturated monolayer on (2√2×√2)R45°-O/Cu(100). Red crosses indicate regular combustion.

RESULTS AND DISCUSSION

The (2√2×√2)R45° superstructure of 1 ML O/Cu(100)[21,22] and the PAHs studied are shown in Figure 1. Those molecules decomposing autocatalytically are marked with green ticks. Those undergoing regular non-autocatalytic combustion are marked with red crosses. For brevity, the saturated oxygen layer is referred to as 'O/Cu'. All molecules are burned by the oxygen of the surface oxide into CO_2 and H_2O. As in the case of TA/Cu(110),[13] the desorption maximum shifts to higher temperatures at higher heating rates (Figure S1).

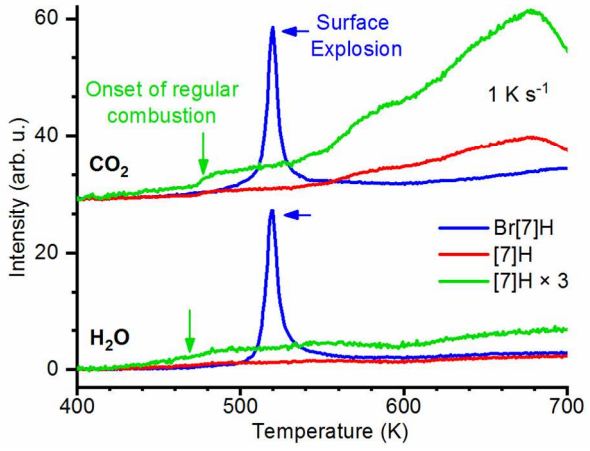

Figure 2. TPR spectra evidencing the decomposition of 1 ML Br[7]H and [7]H on 1 ML O/Cu into CO_2 and H_2O. Br[7]H decomposes in a very narrow temperature window (FWHM 7.5 K) centered at 520 K while [7]H decomposes in a broad temperature range (470 to 670 K). The spectra are offset for clarity.

TPR spectra reveal that saturated monolayers of Br[7]H and [7]H on 1 ML O/Cu combust into CO_2 (44 m/z) and H_2O (18 m/z) (Figure 2). The TPR spectra of [7]H feature broad signals ranging from 470 K to 670 K. In contrast, the spectra of Br[7]H exhibit very narrow (FWHM 7.5 K) peaks at 520 K. Such narrow temperature window is a key signature of surface explosion, which cannot be associated with the simple kinetics of zero, first or second order reactions. XP spectra recorded after TPRS up to 823 K reveal that oxygen and bromine are completely desorbed and that the equivalent of 2/3 of a molecular monolayer of carbon remains on the surface (Figure S2 and S3).

As evident from the TPRS data in Figure 2, the presence or absence of a single Br atom in the molecule is decisive for the reaction pathway: [7]H undergoes regular combustion while Br[7]H combusts autocatalytically. It is known that on native copper surfaces, the C–Br bond in organohalides is dissociated significantly below room temperature and organometallic C–Cu bonds are formed.[23–25] On oxygen covered copper surfaces C–Br bond scission occurs above room temperature,[18,23] for example at 338 K for Br[4]H on O/Cu.[23] For Br[7]H on O/Cu, the onset of C–Br bond scission occurs at 348 K, as indicated by the appearance of a XPS Br $3p_{3/2}$ peak at lower binding energy (Figure 3a). Also, STM data of Br[7]H on O/Cu (Figure 3b) reveals that the molecules appear in pairs after annealing at 348 K (Figure 3c), which strongly suggests the for-

mation of organometallic copper complexes.[23,26] In case of diBr[4]H on O/Cu, the much higher Br/C ratio allows to identify the C–Cu bond formation by C 1s XPS: after annealing at 348 K a low binding energy C 1s signal at 283.2 eV is observed (Figure S4). Such low binding energy C 1s signals are characteristic for organometallic carbon,[27,28] *i.e.* molecules form C–Cu bonds with Cu atoms in the surface layer or with Cu ad-atoms.

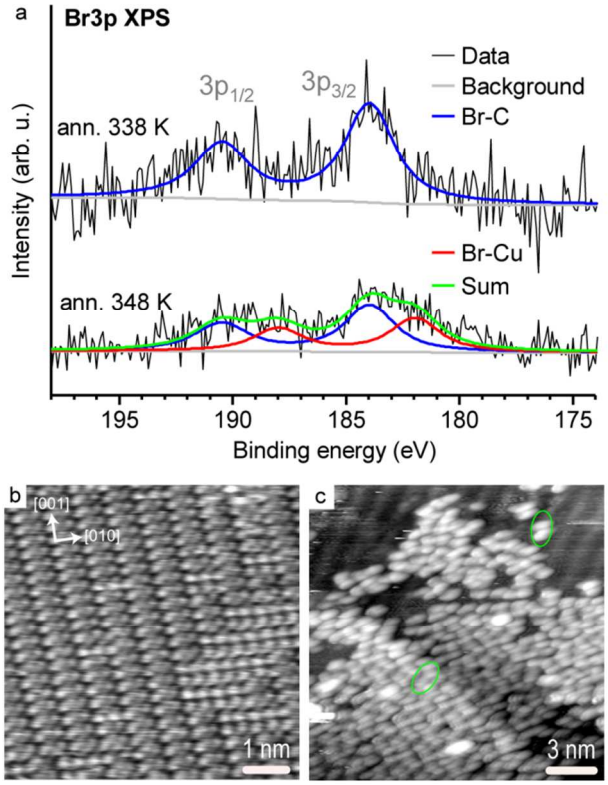

Figure 3. (a) Br 3p XP spectra of 1 ML Br[7]H on O/Cu. After annealing at 348 K, a Br $3p_{3/2}$ XP peak at 181.9 eV appears in addition to the previously present C–Br signal at 183.9 eV, indicating the onset of C–Br bond dissociation. (b) STM image showing the well-defined (2√2×√2)R45° superstructure of 1 ML O/Cu (U = –5 mV, I = –3 nA, T = 295 K).[22] (c) STM image of 0.3 ML Br[7]H on 1 ML O/Cu, annealed to 348 K (U = –3.1 V, I = –160 pA, T = 130 K). The molecules arrange in partly ordered islands consisting of molecular dimers (green ellipses).

As discussed above, the dissociation of Br from Br[7]H occurs at significantly lower temperature than the surface explosion. In the temperature range (400 to 600 K) relevant for surface explosion, the molecules form organometallic bonds with the Cu surface atoms. Note that previous reports showed that the C–C coupling of the Ullmann reaction does not occur on O/Cu surfaces.[18,23,26] In order to exclude any catalytic role of the bromine atoms on the surface, O/Cu was partially covered with bromine and 1 ML [7]H was adsorbed on top of this sample. The absence of surface explosion (Figure S5) confirms that the fixation of debrominated Br[7]H via C–Cu bonds is one of the requirements for surface explosion here.

It has been shown early on that the reaction rate of autocatalytic surface explosion crucially depends on the 'coverage' of vacancies ($1 - \theta$).[13] In contrast to previous studies concerned with molecular layers on bare metal substrates, here vacancies can occur in the oxygen layer as well as in the molecular layer. CO_2 TPR spectra of different molecular coverages (θ_{mol}) of Br[7]H at different oxygen coverages (θ_{ox}) allow to identify which type of vacancies are responsible for the autocatalytic behavior (Figure 4). The complete spectra including the H_2O signals are presented in Figure S6. With decreasing oxygen coverage the TPR peak broadens and its maximum shifts towards lower temperature (Figure 4a). Conversely, with decreasing molecular coverage the TPRS peak remains narrow and shifts slightly towards higher temperatures (Figure 4b). The characteristic behavior of the TPR signals with respect to the oxygen coverage clearly shows that vacancies in the oxygen layer are crucial for autocatalytic decomposition.[13,29]

In order to shine light into the mechanism, TPR spectra were simulated using eq. 2 (Figure 4c-d).

$$r = \theta_{ox}\,{\theta_{mol}}^{1/3}(1-\theta_{ox})\,k_{ex} + \theta_{ox}\,{\theta_{mol}}^{1/3}\,k_{norm} \qquad (2)$$

Here, $r = -\mathrm{d}\theta/\mathrm{d}t$ is proportional to the desorption rates of CO_2 and H_2O. $k_{ex} = \nu_{ex}\exp[-E_A/(RT)]$ and $k_{norm} = \nu_{norm}\exp[-E_A/(RT)]$ are the rate constants for explosive and non-explosive decomposition defined by the attempt frequencies $\nu_{ex} = 10^{15}$ Hz, $\nu_{norm} = 10^{10}$ Hz, the activation energy of the rate limiting step E_A = 150 kJ mol^{-1}, the gas constant R and the temperature T. The non-explosive decomposition channel is required because in its absence, surface explosion cannot start for θ_{ox} = 1 ML.[13,29] The relative rate of non-explosive decomposition defined by the ratio ν_{norm}/ν_{ex} essentially determines the peak width by defining the concentration of vacancies at the onset of surface explosion. Note that in TPRS, E_A and ν are highly interdependent. The simulations allow reproducing the main characteristics of both autocatalytic and regular combustion. Using the same attempt frequency and activation energy, the simulations reproduce i) the TPRS peak for the autocatalytic decomposition of 1 ML Br[7]H on 1 ML oxygen, ii) the shift to lower temperatures as well as the broadening of the TPRS signal with deceasing oxygen coverage, and iii) the fact that the TPRS peaks remain narrow, located at virtually the same temperature, with decreasing molecular coverage.

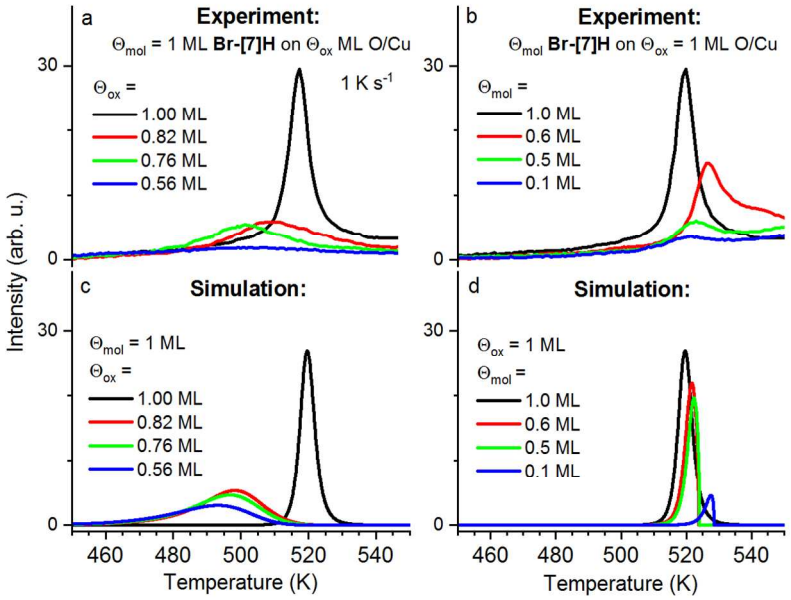

Figure 4. CO_2 TPR spectra of Br[7]H on O/Cu as a function of oxygen (a) and molecular coverage (b). Simulated TPR spectra (c-d). The simulations are preformed using rate equation 2 which involves an autocatalytic $(1 - \theta_{ox})$ term. The model reproduces the main characteristics observed in the experiments, namely: the temperature of the autocatalytic combustion peak and its shift and broadening with decreasing oxygen coverage and the absence of significant broadening and temperature shift with decreasing molecular coverage.

Interestingly, during surface explosion of Br[7]H, the H_2O TPRS signals are observed at lower temperature (*i.e.* before) than the CO_2 signal (Figure 5). It is known that dehydrogenation and cyclodehydrogenation of sterically overcrowded polycyclic aromatic hydrocarbons leads to the formation of C–C bonds and the production of atomic hydrogen.[30–32] Such transiently produced atomic hydrogen has been reported to desorb from O/Cu as H_2O,[33] from Br/Au as HBr,[32] and possibly as HCN from cyano group containing molecules.[34] In the present case, the leading H_2O TPR signal strongly suggests that the atomic hydrogen produced during partial dehydrogenation of sterically overcrowded Br[7]H leads to the desorption of H_2O, thereby creating initial vacancies in the oxygen layer.

The hypothesis that transient atomic hydrogen produced by dehydrogenation of sterically overcrowded PAHs is responsible for the autocatalytic decomposition is tested by studying saturated monolayers of different PAHs (schemes and full names in Figure 1b) on 1 ML O/Cu. Br[4]H, diBr[4]H and diBrbiA decompose autocatalytically yielding narrow TPRS peaks (Figure S7). Indeed, the helicity of the [4]helicenes (Br[4]H and diBr[4]H) is due to strong repulsion between the hydrogen atoms at 1,12 positions (indicated in blue in Figure 1b). Such steric strain imposes higher reactivity for dehydrogenation by favoring C–C bond formation. The same applies to diBrbiA, where C–C bonds between the anthracene units are formed by cyclodehydrogenation.[31] In contast, diBrTP, BrP and diBrA are devoid of steric overcrowding and decompose non-autocatalytically over a wide temperature range, (Figure S8).

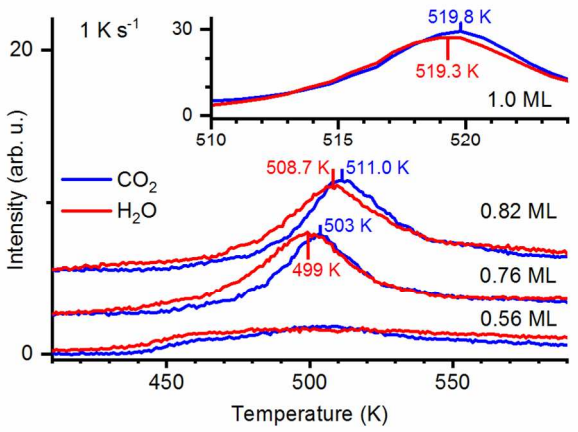

Figure 5. Comparison of CO_2 and H_2O TPR spectra of different molecular coverages of Br[7]H on 1 ML O/Cu. The H_2O signal is always observed at lower temperature than the CO_2 signal. The case of 1 ML Br[7]H on 1 ML O/Cu shown in the inset. The spectra are vertically offset for clarity.

As the case of [7]H shows, steric overcrowding alone is not sufficient for surface explosion. It takes stabilization by a C–surface bond, only obtained from Br-PAH precursors. Without such fixation, the molecules are too weakly adsorbed and are desorbed below reaction temperature is reached. In addition, the autocatalytic process might be facilitated by the organometallic C–Cu bond, which may cause a weakening of adjacent C–C bonds.[35] Once vacancies in the oxygen layer are created, decomposition *via* C–C bond breaking proceeds efficiently catalyzed by the Cu surface atoms. Notably in all reported cases of surface

explosion, the molecules were strongly interacting with the metal substrates.

CONCLUSION

Brominated and bromine-free PAHs on O/Cu(100) decompose into H_2O and CO_2. Saturated monolayers of Br[7]H, Br[4]H, diBr[4]H and diBrbiA decompose autocatalytically in a very narrow temperature range. In contrast, halogen-free [7]H as well as halogen-containing planar diBrTP and diBrA do not decompose autocatalytically. The nature of the autocatalytic mechanism relies on vacancies in the oxygen layer, which are created in the course of the reaction from by dehydrogenation of weakly bonded hydrogen of the PAHs, forming H_2O. Hence, only sterically overcrowded halogenated PAHs, providing such weaker bonded hydrogen, decompose autocatalytically. To our knowledge, this is the first example in which the vacancies in the atomic oxygen layer and not in the molecular layer are explicitly shown to be the chain propagator. Another requirement for surface explosion of PAHs on O/Cu is an organometallic bond formed after C–Br bond scission. These requirements for surface explosion, their modes of action and consequences are summarized in Table 1.

Table 1. Required properties for autocatalytic decomposition

Required Property	Mode of Action	Consequence
Br–R bond in PAH	Organometallic C–Cu bond	Fixation of PAH to surface
Sterically overcrowded PAH	Atomic hydrogen produced at low temperature while C–Cu still intact	Initiation (creation of first vacancies) by desorption of H_2O
Saturated ML of oxygen	Low density of vacancies (active sites)	Exponentially increasing rate of combustion after initiation

The autocatalytic combustion of PAHs on oxygen-covered surfaces is a new type of surface chemistry. In contrast to the previously described surface explosion reactions, it includes the surface coverage of oxygen in the mechanism. Oxygen is a common participant in numerous heterogeneously catalyzed reactions. Therefore, the here described discovery may have implications for better understanding of autocatalytic surface reactions as well a heterogeneous catalysis.

EXPERIMENTAL DETAILS

All experiments have been performed in ultrahigh vacuum ($p < 10^{-9}$ mbar). X-ray photoelectron spectroscopy (XPS) measurements (Specs PHOIBOS 100 electron analyzer) were conducted in normal-emission using non-monochromatic Al K_α X-rays. The binding energy scale was calibrated on the Cu $2p_{3/2}$ peak (932.7 eV) and the Fermi level (0.0 eV) of the Cu(100) crystal. The intensities were normalized with respect to the Cu $2p_{3/2}$ signal. Background spectra obtained on the clean sample were subtracted. Temperature programmed reaction spectroscopy (TPRS) data were obtained using a quadrupole mass spectrometer (Balzers QME 200) at specific masses: 44 m/z (CO_2), 18 m/z (H_2O) and 2 m/z (H_2). Only small amounts of H_2 were detected above 700 K (Figure S9). A special housing (so-called Feulner cup) with a pinhole was installed to avoid collecting material from the sample holder. For each mass spectroscopy channel, the intensity obtained before starting the temperature ramp (which corresponds to the residual partial base pressure of the corresponding gas) was subtracted. Scanning tunneling microscopy (STM) data (Specs Aarhus 150) were recorded in constant current mode with a mechanically cut and in-situ sputtered Pt/Ir (90% Pt) tip. The molecules were synthesized according to refs. 23 (Br[4]H), 36 (diBr[4]H) and 37 ([7]H and Br[7]H). diBrbiA, BrP, diBrTP and diBrA were purchased from Sigma-Aldrich.

The Cu(100) single crystal was prepared via consecutive Ar-sputtering and annealing cycles. The PAH molecules were deposited by sublimation onto the sample kept at room temperature. The coverages of molecules and oxygen were determined from the integrated C 1s and O 1s XPS intensities. The saturated oxygen layer corresponds the nominal oxygen coverage (θ_{ox}) of 1 ML showing a $(2\sqrt{2}\times\sqrt{2})R45°$structure (Figure 3b).[21,22] It was prepared using a partial pressure of $5 \cdot 10^{-6}$ mbar of O_2 at 573 K for 500 s followed by 5 min annealing at 573 K. Lower oxygen coverages were obtained for smaller O_2 doses. Multilayer coverage of Br[7]H, [7]H, Br[4]H, diBr[4]H were desorbed by annealing at 348 K (Br[7]H and [7]H) and 413 K (Br[4]H, diBr[4]H), leaving only molecules in the first layer. The resulting coverage was then assigned to 1 ML. Nominally higher Br[7]H coverages at room temperature did not affect the surface explosion process (Figure S10). For BrP, BrTP, diBrbiA and diBrA, saturation of the coverage was observed at room temperature. Br was deposited on the surface by combustion of Br[7]H at 633 K while dosing O_2 (3×10^{-5} mbar), followed by 5 min annealing at 633 K. The procedure yields a Br doped, carbon-free O/Cu surface (Figure S3).

ASSOCIATED CONTENT

Supporting Information. Additional TPRS and XPS data. This material is available free of charge via the Internet at http://pubs.acs.org.

AUTHOR INFORMATION

Corresponding Author

* E-mail: karl-heinz.ernst@empa.ch
* E-mail: christian.waeckerlin@empa.ch

Funding Sources

University Research Priority Program LightChEC of the University of Zürich, Switzerland
Swiss National Science Foundation (R'Equip and Grant 200020_163296)
Competence Centre for Materials (CCMX), Switzerland

Notes

The authors declare no competing financial interest.

ACKNOWLEDGMENT

Financial support by the University Research Priority Program LightChEC of the University of Zürich, Switzerland, the Swiss National Science Foundation (R'Equip and Grant 200020_163296), and the Competence Centre for Materials (CCMX), Switzerland is gratefully acknowledged. Financial support in France by the CNRS, the University of Angers and the Région Pays de la Loire through the RFI LUMOMAT (grant to K.M.) is acknowledged.

REFERENCES

1. Gadgil, C. J.; Kulkarni, B. D. Autocatalysis in Biological Systems. *AIChE J.* **2009**, *55*, 556–562.
2. McCarty, J.; Falconer, J.; Madix, R. J. Decomposition of Formic Acid on Ni(110): I. Flash Decomposition from the Clean Surface and Flash Desorption of Reaction Products. *J. Catal.* **1973**, *30*, 235–249.
3. Falconer, J.; McCarty, J.; Madix, R. J. The Explosive Decomposition of Formic Acid on Clean Ni(110). *Jpn. J. Appl. Phys.* **1974**, *13*, 525.
4. Gellman, A. J.; Ernst, K.-H. Chiral Autocatalysis and Mirror Symmetry Breaking. *Catal. Lett.* **2018**, *148*, 1610–1621.
5. Yun, Y.; Gellman, A. J. Adsorption-Induced Auto-Amplification of Enantiomeric Excess on an Achiral Surface. *Nat. Chem.* **2015**, *7*, 520–525.
6. Youngs, T. G. A.; Haq, S.; Bowker, M. Formic Acid Adsorption and Oxidation on Cu(110). *Surf. Sci.* **2008**, *602*, 1775–1782.
7. Bowker, M.; Madix, R. XPS, UPS and Thermal Desorption Studies of the Adsorption and Reactions of CH3CHO and CH3COOH with the Cu(110) Surface. *Vacuum* **1981**, *31*, 711–714.
8. Bowker, M.; Madix, R. J. XPS, UPS and Thermal Desorption Studies of the Reactions of Formaldehyde and Formic Acid with the Cu(110) Surface. *Surf. Sci.* **1981**, *102*, 542–565.
9. Bowker, M.; Morgan, C.; Couves, J. Acetic Acid Adsorption and Decomposition on Pd(1 1 0). *Surf. Sci.* **2004**, *555*, 145–156.
10. Aas, N.; Bowker, M. Adsorption and Autocatalytic Decomposition of Acetic-Acid on Pd(110). *J. Chem. Soc.-Faraday Trans.* **1993**, *89*, 1249–1255.
11. Lesley, M. W.; Schmidt, L. D. The NO + CO Reaction on Pt(100). *Surf. Sci.* **1985**, *155*, 215–240.
12. M.W. Lesley; Schmidt, L. D. Chemical Autocatalysis in the NO + CO Reaction on Pt(100). *Chem. Phys. Lett.* **1983**, *102*, 459–463.
13. Mhatre, B. S.; Pushkarev, V.; Holsclaw, B.; Lawton, T. J.; Sykes, E. C. H.; Gellman, A. J. A Window on Surface Explosions: Tartaric Acid on Cu(110). *J. Phys. Chem. C* **2013**, *117*, 7577–7588.
14. Behzadi, B.; Romer, S.; Fasel, R.; Ernst, K. H. Chiral Recognition in Surface Explosion. *J. Am. Chem. Soc.* **2004**, *126*, 9176–9177.
15. Romer, S.; Behzadi, B.; Fasel, R.; Ernst, K.-H. Homochiral Conglomerates and Racemic Crystals in Two Dimensions: Tartaric Acid on Cu(110). *Chem. - Eur. J.* **2005**, *11*, 4149–4154.
16. Sexton, B. A.; Hughes, A. E.; Avery, N. R. A Spectroscopic Study of the Adsorption and Reactions of Methanol, Formaldehyde and Methyl Formate on Clean and Oxygenated Cu(110) Surfaces. *Surf. Sci.* **1985**, *155*, 366–386.
17. Lin, J.-L.; Lin, H.-P.; Yang, C.-M.; Chen, T.-Y.; Lee, S.-H.; Chiang, C.-M. Reactions of CH_2=CHBr and CH_3CHBr_2 on Cu(100) and O/Cu(100). *J. Phys. Chem. C* **2017**, *121*, 17990–17998.
18. Kovács, I. Thermal and Photo-Induced Oxidation of CH2 on Cu(100). *J. Mol. Catal. Chem.* **1999**, *141*, 31–38.
19. Liu, X.; Klust, A.; Madix, R. J.; Friend, C. M. Structure Sensitivity in the Partial Oxidation of Styrene, Styrene Oxide, and Phenylacetaldehyde on Silver Single Crystals. *J. Phys. Chem. C* **2007**, *111*, 3675–3679.
20. Liu, X.; Madix, R. J.; Friend, C. M. Unraveling Molecular Transformations on Surfaces: A Critical Comparison of Oxidation Reactions on Coinage Metals. *Chem. Soc. Rev.* **2008**, *37*, 2243.
21. Kangas, T.; Laasonen, K.; Puisto, A.; Pitkänen, H.; Alatalo, M. On-Surface and Sub-Surface Oxygen on Ideal and Reconstructed Cu(100). *Surf. Sci.* **2005**, *584*, 62–69.
22. Jensen, F.; Besenbacher, F.; Laegsgaard, E.; Stensgaard, I. Dynamics of Oxygen-Induced Reconstruction of Cu(100) Studied by Scanning Tunneling Microscopy. *Phys. Rev. B* **1990**, *42*, 9206–9209.
23. Wäckerlin, C.; Li, J.; Mairena, A.; Martin, K.; Avarvari, N.; Ernst, K.-H. Surface-Assisted Diastereoselective Ullmann Coupling of Bishelicenes. *Chem. Commun.* **2016**, *52*, 12694–12697.
24. Xi, M.; Bent, B. E. Mechanisms of the Ullmann Coupling Reaction in Adsorbed Monolayers. *J. Am. Chem. Soc.* **1993**, *115*, 7426–7433.
25. Dong, L.; Liu, P. N.; Lin, N. Surface-Activated Coupling Reactions Confined on a Surface. *Acc. Chem. Res.* **2015**, *48*, 2765–2774.
26. Fan, Q.; Dai, J.; Wang, T.; Kuttner, J.; Hilt, G.; Gottfried, J. M.; Zhu, J. Confined Synthesis of Organometallic Chains and Macrocycles by Cu–O Surface Templating. *ACS Nano* **2016**, *10*, 3747–3754.
27. Simonov, K. A.; Vinogradov, N. A.; Vinogradov, A. S.; Generalov, A. V.; Zagrebina, E. M.; Svirskiy, G. I.; Cafolla, A. A.; Carpy, T.; Cunniffe, J. P.; Taketsugu, T.; Lyalin, A.; Mårtensson, N.; Preobrajenski, A. B. From Graphene Nanoribbons on Cu(111) to Nanographene on Cu(110): Critical Role of Substrate Structure in the Bottom-Up Fabrication Strategy. *ACS Nano* **2015**, *9*, 8997–9011.
28. Zhang, Y.-Q.; Kepčija, N.; Kleinschrodt, M.; Diller, K.; Fischer, S.; Papageorgiou, A. C.; Allegretti, F.; Björk, J.; Klyatskaya, S.; Klappenberger, F.; Ruben, M.; Barth, J. V. Homo-Coupling of Terminal Alkynes on a Noble Metal Surface. *Nat. Commun.* **2012**, *3*, 1286.
29. Sharpe, R. G.; Bowker, M. Kinetic Models of Surface Explosions. *J. Phys. Condens. Matter* **1995**, *7*, 6379–6392.
30. Stetsovych, O.; Švec, M.; Vacek, J.; Chocholoušová, J. V.; Jančařík, A.; Rybáček, J.; Kosmider, K.; Stará, I. G.; Jelínek, P.; Starý, I. From Helical to Planar Chirality by On-Surface Chemistry. *Nat. Chem.* **2017**, *9*, 213–218.

31. Cai, J.; Ruffieux, P.; Jaafar, R.; Bieri, M.; Braun, T.; Blankenburg, S.; Muoth, M.; Seitsonen, A. P.; Saleh, M.; Feng, X.; Müllen, K.; Fasel, R. Atomically Precise Bottom-up Fabrication of Graphene Nanoribbons. *Nature* **2010**, *466*, 470–473.
32. Bronner, C.; Björk, J.; Tegeder, P.; Bjö Rk, J.; Tegeder, P. Tracking and Removing Br during the On-Surface Synthesis of a Graphene Nanoribbon. *J. Phys. Chem. C* **2015**, *119*, 486–493.
33. Nowakowski, J.; Wäckerlin, C.; Girovsky, J.; Siewert, D.; Jung, T. A.; Ballav, N. Porphyrin Metalation Providing an Example of a Redox Reaction Facilitated by a Surface Reconstruction. *Chem. Commun.* **2013**, *49*, 2347–2349.
34. Rieger, A.; Schnidrig, S.; Probst, B.; Ernst, K.-H.; Wäckerlin, C. Identification of On-Surface Reaction Mechanism by Targeted Metalation. *J. Phys. Chem. C* **2017**, *121*, 27521–27527.
35. Wong, Y.-T.; Hoffmann, R. Theoretical Study of Chemisorption of Acetylene on the Cu(100) Surface. *J. Chem. Soc. Faraday Trans.* **1990**, *86*, 553.
36. Biet, T.; Fihey, A.; Cauchy, T.; Vanthuyne, N.; Roussel, C.; Crassous, J.; Avarvari, N. Ethylenedithio-Tetrathiafulvalene-Helicenes: Electroactive Helical Precursors with Switchable Chiroptical Properties. *Chem. - Eur. J.* **2013**, *19*, 13160–13167.
37. Sudhakar, A.; Katz, T. J. Directive Effect of Bromine on Stilbene Photocyclizations. an Improved Synthesis of [7]Helicene. *Tetrahedron Lett.* **1986**, *27*, 2231–2234.

[TOC graphics]